Composite Structures 136 (2016) 139–148

Contents lists available at ScienceDirect

Composite Structures

journal homepage: www.elsevier.com/locate/compstruct

Domains of dynamic instability of FGM conical shells under time dependent periodic loads

A.H. Sofiyev [a,*], N. Kuruoglu [b]

[a] Department of Civil Engineering of Engineering Faculty of Suleyman Demirel University, Isparta, Turkey
[b] Department of Civil Engineering, Faculty of Engineering and Architecture, Istanbul Gelisim University, Istanbul, Turkey

ARTICLE INFO

Article history:
Available online 22 October 2015

Keywords:
Dynamic instability
Static and dynamic axial load factor
FG conical shell
Domains of instability

ABSTRACT

On the basis of the dynamic version of linear Donnell type equations and with deformations before instability taken into account, the dynamic instability of simply supported, functionally graded (FG) truncated conical shells under static and time dependent periodic axial loads is analyzed. Appling Galerkin's method, the partial differential equations are reduced into a Mathieu-type differential equation describing the dynamic instability behavior of the FG conical shell. The domains of principal instability are determined by using Bolotin's method. Validation of numerical results was done with those available from previous researches. The influences of various parameters like static and dynamic load factors, volume fraction index, FG profiles and shell characteristics on the domains of dynamic instability of conical shell were investigated.

1. Introduction

When in service, the different shell structures or their components may be subjected to periodic loads that somehow change some characteristics of the system. These include, for example, aircrafts with pulsating thrust; underwater pipelines subjected to external pressure and transmitting pulsating flows of oil and gas, mine hoists, which periodically interact with the pit–shaft, etc. The stability problems of such systems under various loads are of interest for reasons of accident prevention. A theoretical analysis of these issues, generally involves solution of nonlinear transient dynamic problems for elastic systems and analysis of various waveforms and scenarios for the emergence of irregular modes. The important dynamic problem of identifying the domains of the instability may be solved in the linear case. This got a boost after Bolotin's [1] contribution to the literature. Bolotin [1] developed the general theory of dynamic instability of elastic systems of deriving the coupled differential equation of the Mathieu-type and the determination of the domains of instability by seeking periodic solution using Fourier series expansion. A comprehensive review of early developments in the dynamic instability of shell elements was presented in the review work by Simitses [2]. Recently, an extensive bibliography of earlier works on dynamic stability/dynamic instability/parametric excitation/parametric resonance of plates and shells was presented by Sahu and Datta [3] from 1987–2005. The dynamic instability of cylindrical shells was adequately studied in Refs. [4–13]. A considerably fewer publications on the dynamic instability are concerned with homogeneous conical shells [14–23]. For example, the approximate solution of the dynamic stability of truncated conical shells under pulsating pressure applying Galerkin and Bolotin method to Donnell type basic equations considering only the transverse inertia term was proposed by Kornecki [14]. The dynamic instability of truncated conical shells under periodic axial loads was studied by Tani [15,16] using the Donnell equations. The dynamic stability of clamped conical shells with variable modulus of elasticity under pulsating torsion excitations was studied using Bolotin's method to obtain the principal instability regions by Massalas et al. [18]. The effects of boundary conditions on the parametric instability of truncated conical shells under periodic edge loading utilizing the generalized differential quadrature (GDQ) method was examined by Ng et al. [19]. The dynamic instability analysis of truncated circular conical shells under periodic in-plane load, was investigated using C^0 two nodded shear flexible shell element by Ganapathia et al. [20]. The WKB (Wentzel, Kramers and Brillouin) method combined with the method of multiple time scales was employed by Kuntsevich and Mikhasev [21] to study the parametric instability for a thin conical shell subjected to non-uniform pulsating pressure. Recently, the parametric resonance of a truncated conical

* Corresponding author at: Department of Civil Engineering of Engineering Faculty of Suleyman Demirel University, 32260 Isparta, Turkey. Tel.: +90 246 211 1195; fax: +90 246 237 0859.

E-mail address: abdullahavey@sdu.edu.tr (A.H. Sofiyev).

http://dx.doi.org/10.1016/j.compstruct.2015.09.060
0263-8223/

shell subjected to periodic axial loads and rotating at periodically varying angular speed based upon the Love's thin shell theory and generalized differential quadrature (GDQ) method was studied by Han and Chu [22,23], respectively.

Recently, a new class of composite materials known as functionally graded materials (FGM) has received considerable attention because of the increasing demands of high structural performance requirements, especially in extreme high-temperature environments and high-speed industries. FGMs are designed to achieve a functional performance with gradually variable properties in one or more spatial directions [24,25]. Noteworthy works considering various aspects of FGM have been published in recent years; see, e.g. [26–28]. In recent years, functionally graded (FG) conical shells are widely used in space vehicles, aircrafts, nuclear power plants and many other engineering applications. Therefore, many studies have been conducted to investigate the static and dynamic behaviors of FG conical shells. A review of the literature shows that the majority of these studies related to the static stability or free vibration analyses of FG conical shells using various shell theories [29–45].

The studies on the dynamic instability analysis of FG shells are much less in comparison to the vibration and static stability. An overview of the works on the subject of dynamic instability of FG shells of various types is mentioned below. Ng et al. [46] examined dynamic instability analysis of FG cylindrical shell subjected under periodic axial loading within the classical shell theory (CST). Ansari and Darvizeh [47] presented a general analytical approach to investigate dynamic behavior of temperature-dependent FG shells under different boundary conditions within the CST. Bespalova and Ursova [48] studied the influence of alternating curvature on the dynamic instability domains of inhomogeneous shells under combined static and dynamic loadings. Ovesy and Fazilati [49] studied a dynamic stability analysis of moderately thick FG cylindrical panels is conducted by employing finite strip formulations. Lei et al. [50] presented a first-known dynamic stability analysis of carbon nanotube-reinforced FG cylindrical panels under static and periodic axial forces by using the mesh-free kp-Ritz method. Torki et al. [51] studied dynamic stability of FG cantilever cylindrical shells under distributed axial follower forces. Sofiyev and Kuruoglu [52] studied the dynamic instability of sandwich cylindrical shells containing an FGM interlayer within classical shell theory (CST). To the best of the authors' knowledge, there is no literature for the solution of dynamic instability analysis of FG truncated conical shells subject to static and time dependent periodic axial load and the authors attempt to fill these apparent voids.

2. Formulation of the problem

The schematic configuration of an FGM truncated conical shell and coordinate system ($S\theta\zeta$) are shown in Fig. 1, where the S-axis in the direction of the generator of the cone, the ζ-axis in the direction normal to the reference surface of the cone, and θ-axis in the direction "perpendicular" to the S–ζ plane. R_1 and R_2 indicate the radii of the cone at its small and large ends, respectively, γ denotes the semi-vertex angle of the cone, L is the length and h is the thickness of the truncated conical shell. The distances along the generator from the apex to the small and large ends of the truncated conical shell are S_1 and $S_2 = S_1 + L$, respectively.

The FG conical shell is assumed to be loaded by static and periodic axial loads [15]:

$$T(t) = T_0 + T_t \cos(Pt) \tag{1}$$

where T_0 is the uniform static axial load, T_t is the amplitude of the periodic axial load, while the frequency P is the frequency of excitation in radians per unit time and t is time variable.

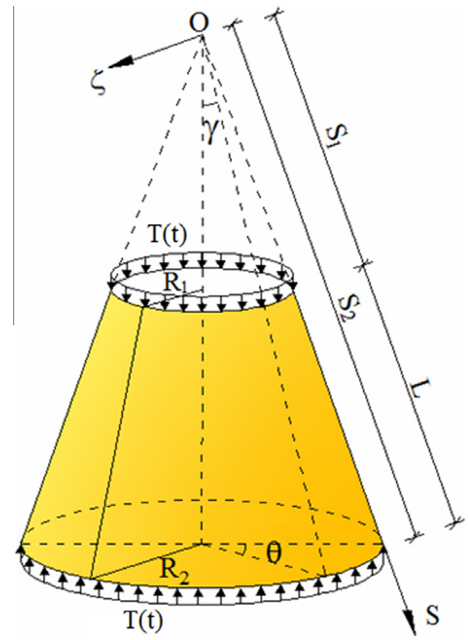

Fig. 1. FG truncated conical shell under time dependent periodic axial load.

The stress state immediately prior to the parametric instability is assumed to be given by the membrane theory as follows:

$$T_S^0 = -T(t), \quad T_\theta^0 = 0; \quad T_{S\theta}^0 = 0 \tag{2}$$

where T_S^0, T_θ^0 and $T_{S\theta}^0$ are the membrane forces for the condition with zero initial moments.

It is assumed that the FGM is made of a mixture of metal and ceramic phases, and the material composition varying smoothly along the axis-ζ, only. The variation of the Young's modulus, Poisson's ratio and density of the FGM conical shell are [53]:

$$\begin{aligned} &E(\zeta_1) = (E_c - E_m)V(\zeta_1) + E_m, \quad \nu(\zeta_1) = (\nu_c - \nu_m)V(\zeta_1) + \nu_m, \\ &\rho(\zeta_1) = (\rho_c - \rho_m)V(\zeta_1) + \rho_m \end{aligned} \tag{3}$$

where E_m, ν_m, ρ_m and E_c, ν_c, ρ_c are the Young's modulus, Poisson's ratio and density of the metal and ceramic surfaces of the FGM shell, respectively, and $\zeta_1 = \zeta/h$. The index "m" represents the metal phase, while the index "c" represents the ceramic phase.

The compositional gradation of the FGM conical shell is defined by the volume fraction of the ceramic phase and the following functions of $V(\zeta_1)$ will be considered [44]:

1. Linear : $\quad V(\zeta_1) = \zeta_1 + 0.5 \quad$ (4.1)
2. Quadratic : $\quad V(\zeta_1) = (\zeta_1 + 0.5)^2 \quad$ (4.2)
3. Inverse Quadratic : $\quad V(\zeta_1) = 1 - (0.5 - \zeta_1)^2 \quad$ (4.3)

3. Basic equations

In the present study, the conical shells are assumed to be thin and the classical shell theory based on Love's hypotheses is used to investigate the dynamic instability of FGM conical shells under static and time dependent periodic axial load. The stress–strain relations of FG truncated conical shells within the classical shell theory are given as [43]:

$$\begin{bmatrix} \sigma_S \\ \sigma_\theta \\ \sigma_{S\theta} \end{bmatrix} = \begin{bmatrix} Q_{11}(\zeta_1) & Q_{12}(\zeta_1) & 0 \\ Q_{12}(\zeta_1) & Q_{11}(\zeta_1) & 0 \\ 0 & 0 & Q_{66}(\zeta_1) \end{bmatrix} \begin{bmatrix} \varepsilon_S \\ \varepsilon_\theta \\ \varepsilon_{S\theta} \end{bmatrix} \tag{5}$$

where $\sigma_S,\ \sigma_\theta,\ \sigma_{S\theta}$ and $\varepsilon_S,\ \varepsilon_\theta,\ \varepsilon_{S\theta}$ are the strains and stresses of the FG conical shell, respectively and the quantities $Q_{ij}(i,j=1,2,6)$ are functions of non-dimensional thickness coordinate, ζ_1, and are expressed as:

$$Q_{11}(\zeta_1)=\frac{(E_c-E_m)V(\zeta_1)+E_m}{1-[(\nu_c-\nu_m)V(\zeta_1)+\nu_m]^2},$$
$$Q_{12}(\zeta_1)=\frac{[(\nu_c-\nu_m)V(\zeta_1)+\nu_m][(E_c-E_m)V(\zeta_1)+E_m]}{1-[(\nu_c-\nu_m)V(\zeta_1)+\nu_m]^2}, \tag{6}$$
$$Q_{66}(\zeta_1)=\frac{(E_c-E_m)V(\zeta_1)+E_m}{1+[(\nu_c-\nu_m)V(\zeta_1)+\nu_m]}$$

According to classical shell theory, the strains across the FG truncated conical shell thickness at a distance ζ from the middle surface are [54]:

$$\begin{bmatrix}\varepsilon_S\\ \varepsilon_\theta\\ \varepsilon_{S\theta}\end{bmatrix}=\begin{bmatrix}\varepsilon_S^0-\zeta\frac{\partial^2 w}{\partial S^2}\\ \varepsilon_\theta^0-\zeta\left(\frac{1}{S^2}\frac{\partial^2 w}{\partial\varphi^2}+\frac{1}{S}\frac{\partial w}{\partial S}\right)\\ \varepsilon_{S\theta}^0-\zeta\left(\frac{1}{S}\frac{\partial^2 w}{\partial S\partial\varphi}-\frac{1}{S^2}\frac{\partial w}{\partial\varphi}\right)\end{bmatrix} \tag{7}$$

where $\varphi=\theta\sin\gamma$ and $\varepsilon_S^0,\ \varepsilon_\theta^0,\ \varepsilon_{S\theta}^0$ are strains on the middle surface.

The force and moment resultants of an FG truncated conical shell are expressed in terms of the stress components through the thickness as [54]:

$$(T_S,T_\theta,T_{S\theta},M_S,M_\theta,M_{S\theta})=\int_{-h/2}^{h/2}[\sigma_S,\sigma_\theta,\sigma_{S\theta},\zeta\sigma_S,\zeta\sigma_\theta,\zeta\sigma_{S\theta}]d\zeta \tag{8}$$

where, $T_S,\ T_\theta,\ T_{S\theta}$ and $M_S,\ M_\theta,\ M_{S\theta}$ are the basic components of stress resultants and stress couples, respectively.

The governing differential equations, given by Agamirov [54] for dynamic instability of conical shells modified for the parametric excitation of FG conical shells can be expressed as:

$$\frac{\partial^2 M_S}{\partial S^2}+\frac{2}{S}\frac{\partial M_S}{\partial S}+\frac{2}{S}\frac{\partial^2 M_{S\theta}}{\partial S\partial\varphi}-\frac{1}{S}\frac{\partial M_\theta}{\partial S}+\frac{2}{S^2}\frac{\partial M_{S\theta}}{\partial\varphi}+\frac{1}{S^2}\frac{\partial^2 M_\theta}{\partial\varphi^2}+\frac{T_\theta}{S}\cot\gamma$$
$$-\frac{[T_0+T_t\cos(Pt)]}{S}\left(\frac{1}{S}\frac{\partial^2 w}{\partial\varphi^2}+\frac{\partial w}{\partial S}\right)=\rho_t\frac{\partial^2 w}{\partial t^2} \tag{9}$$

$$\frac{\cot\gamma}{S}\frac{\partial^2 w}{\partial S^2}-\frac{2}{S}\frac{\partial^2\varepsilon_{S\theta}^0}{\partial S\partial\varphi}-\frac{2}{S^2}\frac{\partial\varepsilon_{S\theta}^0}{\partial\varphi}+\frac{\partial^2\varepsilon_\theta^0}{\partial S^2}+\frac{1}{S^2}\frac{\partial^2\varepsilon_S^0}{\partial\varphi^2}+\frac{2}{S}\frac{\partial\varepsilon_\theta^0}{\partial S}-\frac{1}{S}\frac{\partial\varepsilon_S^0}{\partial S}=0 \tag{10}$$

where ρ_t is a parameter of density and the following notation applies:

$$\rho_t=\int_{-h/2}^{h/2}[(\rho_c-\rho_m)V_c(\zeta_1)+\rho_m]d\zeta_1 \tag{11}$$

The connections of forces with the undetermined Airy stress function, $\Psi(S,\theta,t)$, are given by the following relations [54]

$$(T_S,T_\theta,T_{S\theta})=h\left(\frac{1}{S^2}\frac{\partial^2\Psi}{\partial\varphi^2}+\frac{1}{S}\frac{\partial\Psi}{\partial S},\frac{\partial^2\Psi}{\partial S^2},-\frac{1}{S}\frac{\partial^2\Psi}{\partial S\partial\varphi}+\frac{1}{S^2}\frac{\partial\Psi}{\partial\varphi}\right) \tag{12}$$

Substituting (7) into the constitutive law (5) and considering the resulting expressions in the Eqs. (8), after some rearrangements the expressions found for moments and strains, being substituted in the Eqs. (9) and (10), together with the relation (12), then considering the variable $S=S_1e^z$ and $\Psi=\Psi_1e^{2z}$ is taken into account instead of Ψ, after lengthy computations, the system of linear partial differential equations for Ψ_1 and w can be written as:

$$c_2e^{2z}\left(\frac{\partial^4\Psi_1}{\partial z^4}-4\frac{\partial^3\Psi_1}{\partial z^3}+4\frac{\partial^2\Psi_1}{\partial z^2}+\frac{\partial^4\Psi_1}{\partial\varphi^4}+2\frac{\partial^2\Psi_1}{\partial\varphi^2}\right)$$
$$+2(c_1-c_5)e^{2z}\left(\frac{\partial^4\Psi_1}{\partial z^2\partial\varphi^2}-2\frac{\partial^3\Psi_1}{\partial z\partial\varphi^2}+\frac{\partial^2\Psi_1}{\partial\varphi^2}\right)$$
$$+\left(\frac{\partial^2\Psi_1}{\partial z^2}+3\frac{\partial\Psi_1}{\partial z}+2\Psi_1\right)S_1e^{3z}\cot\gamma$$
$$-c_3\left(\frac{\partial^4 w}{\partial\varphi^4}+\frac{\partial^4 w}{\partial z^4}-4\frac{\partial^3 w}{\partial z^3}+4\frac{\partial^2 w}{\partial z^2}+2\frac{\partial^2 w}{\partial\varphi^2}\right)$$
$$-2(c_4+c_6)\left(\frac{\partial^4 w}{\partial z^2\partial\varphi^2}-2\frac{\partial^3 w}{\partial z\partial\varphi^2}+\frac{\partial^2 w}{\partial\varphi^2}\right)$$
$$-[T_0+T_t\cos(Pt)]S_1^2e^{2z}\left(\frac{\partial^2 w}{\partial z^2}-\frac{\partial w}{\partial z}\right)-\rho_tS_1^4e^{4z}\frac{\partial^2 w}{\partial t^2}=0 \tag{13}$$

$$b_1e^{2z}\left(\frac{\partial^4\Psi_1}{\partial z^4}-4\frac{\partial^3\Psi_1}{\partial z^3}+4\frac{\partial^2\Psi_1}{\partial z^2}+\frac{\partial^4\Psi_1}{\partial\varphi^4}+2\frac{\partial^2\Psi_1}{\partial\varphi^2}\right)$$
$$+2(b_5+b_2)e^{2z}\left(\frac{\partial^4\Psi_1}{\partial z^2\partial\varphi^2}-2\frac{\partial^3\Psi_1}{\partial z\partial\varphi^2}+\frac{\partial^2\Psi_1}{\partial\varphi^2}\right)$$
$$-b_4\left(\frac{\partial^4 w}{\partial\varphi^4}+2\frac{\partial^2 w}{\partial\varphi^2}+\frac{\partial^4 w}{\partial z^4}-4\frac{\partial^3 w}{\partial z^3}+4\frac{\partial^2 w}{\partial z^2}\right)$$
$$+2(b_6-b_3)\left(\frac{\partial^4 w}{\partial z^2\partial\varphi^2}-2\frac{\partial^3 w}{\partial z\partial\varphi^2}+\frac{\partial^2 w}{\partial\varphi^2}\right)$$
$$+\left(\frac{\partial^2 w}{\partial z^2}-\frac{\partial w}{\partial z}\right)S_1e^z\cot\gamma=0 \tag{14}$$

Here, we introduce the following quantities:

$$c_1=a_{11}b_1+a_{21}b_2,\quad c_2=a_{11}b_2+a_{21}b_1,\quad c_3=a_{11}b_3+a_{21}b_4+a_{12},$$
$$c_4=a_{11}b_4+a_{21}b_3+a_{22},$$
$$c_5=a_{61}b_5,\quad c_6=a_{61}b_6+a_{62},\quad b_1=a_{10}/L_0,\quad b_2=-a_{20}/L_0,$$
$$b_3=(a_{20}a_{21}-a_{11}a_{10})/L_0,$$
$$b_4=(a_{20}a_{11}-a_{21}a_{10})/L_0,\quad b_5=1/a_{60},\quad b_6=-a_{61}/a_{60},$$
$$L_0=(a_{10})^2-(a_{20})^2 \tag{15}$$

in which expressions $a_{ik},\ (i=1,2,6;k=0,1,2)$ are defined as follows:

$$a_{1k}=\int_{-h/2}^{h/2}\zeta^k\frac{(E_c-E_m)V(\zeta_1)+E_m}{1-[(\nu_c-\nu_m)V(\zeta_1)+\nu_m]^2}d\zeta,$$
$$a_{2k}=\int_{-h/2}^{h/2}\zeta^k\frac{[(E_c-E_m)V(\zeta_1)+E_m][(\nu_c-\nu_m)V(\zeta_1)+\nu_m]}{1-[(\nu_c-\nu_m)V(\zeta_1)+\nu_m]^2}d\zeta \tag{16}$$
$$a_{6k}=\int_{-h/2}^{h/2}\zeta^k\frac{(E_c-E_m)V(\zeta_1)+E_m}{1+(\nu_c-\nu_m)V(\zeta_1)+\nu_m}d\zeta$$

The Eqs. (13) and (14) can be used for the study of the dynamic instability of FG truncated conical shells under time dependent periodic axial load.

4. Solution of basic equations

The FG truncated conical shell is assumed to be simply supported at $S=S_1$ and $S=S_2$, thus the solution of Eq. (14) is sought in the following form as [54]:

$$w=f(t)e^z\sin(m_1z)\sin(m_2\varphi) \tag{17}$$

where $f(t)$ is time dependent unknown function and the following definitions are introduced:

$$m_1 = \frac{m\pi}{z_0}, \quad m_2 = \frac{n}{\sin\gamma}, \quad z_0 = \ln\frac{S_2}{S_1} \tag{18}$$

Substituting Eq. (17) into Eq. (14) and by applying the Superposition principle can be obtained as:

$$\Psi_1 = f(t)[K_1\sin(m_1 z) + K_2\cos(m_1 z) + K_3 e^{-z}\sin(m_1 z) + K_4 e^{-z}\cos(m_1 z)]\sin(m_2\varphi) \tag{19}$$

where the following definitions apply:

$$K_1 = \frac{m_1(m_1 q_0 + q_2)S_1\cot\gamma}{q_0^2 + q_2^2}, \quad K_2 = \frac{m_1(m_1 q_2 - q_0)S_1\cot\gamma}{q_0^2 + q_2^2},$$
$$K_3 = \frac{q_3 q_1}{q_1^2 + q_4^2}, \quad K_4 = -\frac{q_3 q_4}{q_1^2 + q_4^2} \tag{20}$$

in which

$$\begin{aligned} q_0 &= b_1(m_2^4 - 3m_1^2) + 2(b_5 + b_2)m_1^2 m_2^2 - 2(b_5 + b_2 + b_1)m_2^2, \\ q_1 &= 2(b_5 + b_2)m_1^2 m_2^2 + b_1(m_1^4 + m_2^4 + 2m_1^2 - 2m_2^2 + 1), \\ q_2 &= 4b_1 m_1^3 + 4(b_5 + b_2)m_1 m_2^2, \\ q_3 &= b_4[(m_2^2 - 1)^2 + m_1^2] + m_1^2[2(b_3 - b_6)m_2^2 + b_4(m_1^2 + 1)], \\ q_4 &= -8(b_5 + b_2)m_1 m_2^2 + 24 b_1 m_1 - 8 b_1 m_1^3 \end{aligned} \tag{21}$$

Substituting Eqs. (14) and (19) into the Eq. (13), then applying the Galerkin method to the resulting equations in the ranges $0 \leqslant \varphi \leqslant 2\pi\sin\gamma$ and $0 \leqslant z \leqslant z_0$, and after integration and some mathematical operations one gets

$$\frac{d^2 f(t)}{dt^2} + \frac{\Lambda_1 + \Lambda_2 + \Lambda_3 + \Lambda_4 - \Lambda_6[T_{0ax} + T_{tax}\cos(Pt)]}{\Lambda_5\rho_t} f(t) = 0 \tag{22}$$

where the following quantities are introduced:

$$\Lambda_1 = \begin{bmatrix} c_2(K_1 m_1^4 + 4K_2 m_1^3 - 4K_1 m_1^2 + K_1 m_2^4 - 2K_1 m_2^2) \\ +2(c_1 - c_5)m_2^2(2K_2 m_1 - K_1 + K_1 m_1^2) - (K_3 m_1^2 + K_4 m_1)S_1\cot\gamma \end{bmatrix} \frac{2m_1^2(1 - e^{3z_0})}{3(4m_1^2 + 9)},$$
$$\Lambda_2 = \begin{bmatrix} c_2(K_3 m_1^4 + 2K_3 m_1^2 + K_3 + K_3 m_2^4 - 2K_3 m_2^2) + 2(K_3 m_1 - K_4)m_1 m_2^2 \\ \times(c_1 - c_5) - c_3(m_1^4 + 2m_1^2 + m_2^4 - 2m_2^2 + 1) - 2m_1^2 m_2^2(c_4 + c_6) \end{bmatrix} \frac{m_1^2(1 - e^{2z_0})}{4(m_1^2 + 1)},$$
$$\Lambda_3 = \begin{bmatrix} c_2(K_2 m_1^4 - 4K_1 m_1^3 - 4K_2 m_1^2 + K_2 m_2^4 - 2K_2 m_2^2) \\ -2(c_1 - c_5)m_2^2(K_2 - K_2 m_1^2 + 2K_1 m_1) + (K_3 m_1 - K_4 m_1^2)S_1\cot\gamma \end{bmatrix} \frac{m_1(e^{3z_0} - 1)}{4m_1^2 + 9},$$
$$\Lambda_4 = \frac{(K_2 + K_1 m_1)m_1}{8}(e^{4z_0} - 1)S_1\cot\gamma, \quad \Lambda_5 = \frac{m_1^2(e^{6z_0} - 1)S_1^4}{12(m_1^2 + 9)}, \quad \Lambda_6 = \frac{S_1^2 m_1^2(2 + m_1^2)(e^{4z_0} - 1)}{8(m_1^2 + 4)} \tag{23}$$

The Eq. (22) represents those for static axial buckling and free vibration of FG truncated conical shells, as special cases.

If the axial load is not included in the Eq. (22), we obtain the expressions for the dimensional and dimensionless frequencies of FG truncated conical shells:

$$\omega = \sqrt{\frac{\Lambda_1 + \Lambda_2 + \Lambda_3 + \Lambda_4}{\Lambda_5\rho_t}} \tag{24}$$

and

$$\omega_1 = R_1\omega\sqrt{\frac{(1 - \nu_c^2)\rho_c}{E_c}} \tag{25}$$

If the inertial term is not included in the Eq. (22), we obtain the expressions for dimensional and dimensionless static critical axial loads for FG truncated conical shells:

$$T_{cr}^{st} = \frac{\Lambda_1 + \Lambda_2 + \Lambda_3 + \Lambda_4}{\Lambda_6} \tag{26}$$

and

$$T_{1cr}^{st} = \frac{T_{cr}^{st}}{E_c h} \tag{27}$$

To find the minimum values of dimensional and dimensionless static critical axial loads and frequencies of FG truncated conical shells, Eqs. (24)–(27) are minimized in accordance with the wave numbers (m, n).

Transform the Eq. (22) in the form of a second order differential equation with time-dependent periodic coefficient:

$$\frac{d^2 f(t)}{dt^2} + \omega^2[1 - T_{01} - T_{t1}\cos(Pt)]f(t) = 0 \tag{28}$$

where $T_{01} = \frac{T_0}{T_{cr}^{st}}$ is a static axial load factor and $T_{t1} = \frac{T_t}{T_{cr}^{st}}$ is a dynamic axial load factor for FG truncated conical shells.

The above Eq. (22) is a differential equation with the periodic coefficient, such as Mathieu-type equation. The boundaries of primary instability regions of the period 2T, where $T = 2\pi/P$ is of great practical importance, since the width of these unstable regions are generally higher than those associated with the solutions that have a period "T". The principal instability domains in which the solution of Eq. (22) becomes unstable are determined by means of Bolotin's method. The solutions of period $2T$ ($T = 2\pi/P$), which correspond to the boundaries of domains of principal instability, can be achieved in the form of the trigonometric series

$$f(t) = \sum_{i=1,3,5,\ldots}^{\infty} \bar{a}_i\cos\left(\frac{Pt}{2}\right) + \bar{b}_i\sin\left(\frac{Pt}{2}\right) \tag{29}$$

where $\bar{a}_i$ and $\bar{b}_i$ are unknown parameters.

Introducing of (29) into Eq. (22) and if only first term of the series is considered, then discarding terms with the triple frequency from the resulting equation, the Eq. (22) reduces to

$$[-P^2 + 4\omega^2(1 - T_{01} - 0.5T_{t1})]\bar{a}_1\cos\left(\frac{Pt}{2}\right) + [-P^2 + 4\omega^2(1 - T_0 + 0.5T_{t1})]\bar{b}_1\sin\left(\frac{Pt}{2}\right) = 0 \tag{30}$$

Eq. (30) can be used to obtain the excitation frequencies, i.e., the boundaries of domains of principal instability of FG truncated conical shells.

As $\bar{a}_1 \neq 0$ and $\bar{b}_1 \neq 0$, from Eq. (30), we obtain the expression for the dimensionless excitation frequencies of parametric vibration or for boundaries of domains of principal instability of FG truncated conical shells, respectively,

$$p_{1j} = 4\pi\omega_1\sqrt{1 - T_{01} \mp 0.5T_{t1}}, \quad (j = 1,2) \tag{31}$$

where p_{1j}, $(j = 1,2)$ are the dimensionless excitation frequencies, sign $(-)$ is used as $j = 1$ and sign $(+)$ is used as $j = 2$, and the following definition applies:

$$p_{1j} = 2\pi R_1 P_{1j}\sqrt{(1 - \nu_c^2)\rho_c/E_c}, \quad (j = 1,2) \tag{32}$$

By using Eq. (32) will be found the boundaries between the stable and unstable domains of FG truncated conical shells.

As $T_{t1} = 0$, from Eq. (32) the expression for the point of origin of domains of principal instability of FG truncated conical shells.

If $\gamma \to 0,\ S_1 \to \infty,\ S_1 \sin\gamma = R,\ m_1 \sin\gamma = \frac{m\pi R}{L} = m_3,\ S_2 = S_1 + L$, $z_0 = \ln\frac{S_2}{S_1} = \ln\left(1 + \frac{L}{S_1}\right) \approx \frac{L}{S_1},\ e^{-az_0} \approx 1 - a\frac{L}{S_1},\ a > 0$ are substituted in Eqs. (24), (26) and (32) corresponding formulas for FG cylindrical shells are obtained.

5. Results and discussion

In this section, two comparative studies and the new numerical analysis for the dynamic instability of FG truncated conical shells are presented using Maple 14 software.

5.1. Verification

In order to validate the present study, our results are compared with the results published in the literature.

In first example, the values of origin of domains of principal instability for FG cylindrical shells presented in Table 1 and are compared with those of Ng et al. [46]. In comparison, is used a special case of the expression (32) for the FG cylindrical shell. The volume fraction of FG profile is a linear function. The cylindrical shell characteristics are taken to be $L_1/R = 1$ and $R/h = 100$. The FG cylindrical shell is considered to be silicon nitride and nickel. The Young's moduli of metal and ceramic surfaces of FG cylindrical shells are $E_m = 2.05098 \times 10^{11}$(Pa) and $E_c = 3.2227 \times 10^{11}$(Pa), respectively. The densities and Poisson's ratios of nickel and silicon nitride are 8900 kg/m^3 and 0.24, and 2370 kg/m^3 and 0.31, respectively, which is taken from study of Ng et al. [46]. It is assumed that the dynamic load factor is equal to zero and the constant part of the axial load is certain, i.e. $T_{01} = 0.5$. Two typical modes (1,1) and (1,2) are considered. The values of origin of domains of principal instability for FG cylindrical shells for from present study are compared with those of Ng et al. [46] as shown in Table 1, wherein good agreement is witnessed.

In second example, the values of the dimensionless frequency parameter, ω_1, for the pure metal truncated conical shell are compared with the studies of Li et al. [55] and Kerboua et al. [56] and are presented in Table 2. The material and geometric properties of the pure metal truncated conical shell are: $\nu_{0m} = 0.3$; $R_2/h = 100$; $L = 0.25S_2$; $\gamma = 30^\circ$. As $V_c = 0$, the FG truncated conical shell transformed to the metal truncated conical shell. The present results show good agreement with the results presented by Li et al. [55] and Kerboua et al. [56].

Table 1
Comparison of dimensionless values of origin of domains of principal instability for FG cylindrical shells with those of Ng et al. [46].

$p_{11} = p_{12}$ (m,n)	
Ng et al. [46]	Present study
10.565 (1,1)	10.948 (1,1)
8.081 (1,2)	8.593 (1,2)

Table 2
Comparison of dimensionless frequency parameter of free vibration for the pure metal conical shell.

n	$\omega_1 = \omega R_2\sqrt{(1-\nu_{0m}^2)\rho_{0m}/E_{0m}}$		
	Li et al. [55]	Kerboua et al. [56]	Present study
2	0.8431	0.7909	0.8555
3	0.7416	0.7282	0.7507
4	0.6419	0.6349	0.6470
5	0.5590	0.5525	0.5606
6	0.5008	0.4940	0.5002
7	0.4701	0.4641	0.4695
8	0.4687	0.4631	0.4682

5.2. Effects of system parameters upon instability domains of FG conical shells

After checking the validity of the present study for simply supported metal-rich, ceramic-rich and FG shells subjected to static and time dependent periodic axial load, the new analysis is presented to study the effects of different parameters like the FG profiles, the static and dynamic axial load factors, the radius-to-thickness ratio, the length-to-radius radio and the semi-vertex angle on the dynamic instability behavior of the conical shells. We use the Eq. (32) to find the values of boundaries of domains of dynamic instability applying Maple 14 software. The truncated conical shells that consist of four kinds of functional graded materials are designed as follows:

SUS304/Si_3N_4 or FG-A,
Ti6Al4V/Si_3N_4 or FG-B,
SUS304/FG-C/ZrO_2 or FG-C,
Ti-6Al-4V/ZrO_2 or FG-D.

The material properties of ceramic and metals are assumed to be temperature-dependent according to a nonlinear function as:

$$P = P_0P_{-1}T^{-1} + P_0 + P_0P_1T + P_0P_2T^2 + P_0P_3T^3 \tag{34}$$

where $P_{-1};\ P_0;\ P_1;\ P_2;\ P_3$ are the coefficients of temperature T (K). The material properties are calculated at $T = 300$ K. Typical values for effective Young's modulus E_f (in Pa), Poisson's ratio ν_f and density ρ_f (kg/m^3) of ceramic and metals are listed in Table 3 [53].

Here $E_0,\ \nu_0,\ \rho_0$ are Young's modulus (in Pa), Poisson's ratio and density (kg/m^3) of the pure ceramic or pure metals. Typical results are shown in Table 4 and Figs. 2–5 for different kinds of FG truncated conical shells. The results for FG truncated conical shells are compared with those of ceramic-rich and metal-rich conical shells by estimating the percentage differences of dimensionless values of boundaries of domains of dynamic instability, respectively, as

$$\frac{p_{1j}^{FG} - p_{1j}^{H}}{p_{1j}^{H}} \times 100\%, \quad (j = 1,2).$$

5.2.1. Effect of FG profiles depending on the dynamic axial load factor

The variation of magnitudes of boundaries of instability domains of four kinds FG conical shells, and SUS304, Ti6Al4V, Si_3N_4 and ZrO_2 homogeneous conical shells versus the dynamic axial load factor, $T_{t1} = T_t/T_{cr}$ are computed and tabulated in Table 4. The geometrical characteristics of FG and pure ceramic and metals conical shells are taken to be $R_1/h = 100$; $L/R_1 = 2$;

Table 3
Effective material properties for ceramic and metals.

Coefficients	Si_3N_4			Stainless steel (SUS304)		
	E_c (Pa)	ν_c	ρ_c (kg/m^3)	E_m (Pa)	ν_m	ρ_m (kg/m^3)
(E_0, ν_0, ρ_0)	3.4843×10^{11}	0.24	2370	2.0104×10^{11}	0.3262	8166
(E_f, ν_f, ρ_f)	3.2227×10^{11}	0.24	2370	2.07788×10^{11}	0.317756	8166
	ZrO_2			Ti-6Al-4V		
(E_0, ν_0, ρ_0)	2.4427×10^{11}	0.2882	5680	1.2256×10^{11}	0.2884	4420
(E_f, ν_f, ρ_f)	1.68063×10^{11}	0.298	5680	1.056982×10^{11}	0.2981	4420

Table 4
Variation of the values of boundaries of domains of dynamic instability of FG truncated conical shells versus the dynamic axial load factor, T_{t1}.

(m,n)	T_{t1}	SUS304		FG-A-linear		FG-A-quad.		FG-A-inv. quad.		Si_3N_4	
		p_{11}	p_{12}	p_{11}	p_{12}	p_{11}	p_{12}	p_{11}	p_{12}	p_{11}	p_{12}
(1,1)	0	3.369	3.369	2.249	2.249	1.992	1.992	2.577	2.577	3.695	3.695
	0.2	3.350	3.388	2.237	2.262	1.981	2.003	2.562	2.591	3.674	3.715
	0.4	3.331	3.406	2.224	2.274	1.970	2.014	2.548	2.605	3.653	3.735
(1,2)	0	2.866	2.866	1.915	1.915	1.696	1.696	2.194	2.194	3.143	3.143
	0.2	2.850	2.882	1.905	1.926	1.687	1.706	2.182	2.206	3.125	3.160
	0.4	2.834	2.898	1.894	1.936	1.677	1.715	2.170	2.218	3.108	3.177
(1,3)	0	2.096	2.096	1.404	1.404	1.244	1.244	1.608	1.608	2.298	2.298
	0.2	2.084	2.107	1.396	1.412	1.237	1.251	1.599	1.617	2.285	2.310
	0.4	2.072	2.119	1.389	1.420	1.230	1.258	1.590	1.626	2.272	2.323
		Ti6Al4V		FG-B-linear		FG-B-quad.		FG-B-inv. quad.		Si_3N_4	
(1,1)	0	3.266	3.266	2.517	2.517	2.187	2.187	2.869	2.869	3.695	3.695
	0.2	3.248	3.284	2.503	2.531	2.175	2.200	2.853	2.885	3.674	3.715
	0.4	3.229	3.302	2.489	2.544	2.163	2.212	2.837	2.900	3.653	3.735
(1,2)	0	2.778	2.778	2.145	2.145	1.865	1.865	2.444	2.444	3.143	3.143
	0.2	2.763	2.794	2.133	2.156	1.854	1.875	2.430	2.457	3.125	3.160
	0.4	2.747	2.809	2.121	2.168	1.844	1.885	2.416	2.471	3.108	3.177
(1,3)	0	2.031	2.031	1.574	1.574	1.370	1.370	1.793	1.793	2.298	2.298
	0.2	2.020	2.043	1.566	1.583	1.363	1.378	1.783	1.803	2.285	2.310
	0.4	2.009	2.054	1.557	1.592	1.355	1.385	1.773	1.813	2.272	2.323
		SUS304		FG-C-linear		FG-C-quad.		FG-C-inv. quad.		ZrO_2	
(m,n)	T_{t1}	P_{11}	P_{12}	P_{11}	P_{12}	P_{11}	P_{12}	P_{11}	P_{12}	P_{11}	P_{12}
(1,1)	0	3.369	3.369	3.480	3.480	3.439	3.439	3.525	3.525	3.633	3.633
	0.2	3.350	3.388	3.461	3.499	3.420	3.459	3.506	3.545	3.613	3.653
	0.4	3.331	3.406	3.441	3.519	3.401	3.477	3.486	3.564	3.592	3.673
(1,2)	0	2.866	2.866	2.960	2.960	2.925	2.925	2.998	2.998	3.090	3.090
	0.2	2.850	2.882	2.943	2.976	2.909	2.941	2.982	3.015	3.073	3.107
	0.4	2.834	2.898	2.927	2.993	2.893	2.958	2.965	3.032	3.056	3.124
(1,3)	0	2.096	2.096	2.163	2.163	2.138	2.138	2.192	2.192	2.260	2.260
	0.2	2.084	2.107	2.151	2.175	2.126	2.150	2.179	2.204	2.247	2.272
	0.4	2.072	2.119	2.139	2.187	2.114	2.162	2.167	2.216	2.234	2.285
		Ti6Al4V		FG-D-linear		FG-D-quad.		FG-D-inv. quad.		ZrO_2	
(1,1)	0	3.266	3.266	3.477	3.477	3.414	3.414	3.534	3.534	3.633	3.633
	0.2	3.248	3.284	3.458	3.496	3.395	3.433	3.514	3.554	3.613	3.653
	0.4	3.229	3.302	3.438	3.516	3.376	3.452	3.495	3.573	3.592	3.673
(1,2)	0	2.778	2.778	2.960	2.960	2.907	2.907	3.008	3.008	3.090	3.090
	0.2	2.763	2.794	2.943	2.976	2.890	2.923	2.991	3.025	3.073	3.107
	0.4	2.747	2.809	2.927	2.993	2.874	2.939	2.974	3.041	3.056	3.124
(1,3)	0	2.031	2.031	2.167	2.167	2.129	2.129	2.202	2.202	2.260	2.260
	0.2	2.020	2.043	2.155	2.179	2.117	2.141	2.190	2.214	2.247	2.272
	0.4	2.009	2.054	2.143	2.191	2.105	2.152	2.178	2.227	2.234	2.285

$\gamma = 30^\circ$. Three typical modes $(m,n) = (1,1), (1,2), (1,3)$ are considered and the constant part of the axial load is certain, i.e. $T_{01} = 0.1$. The volume fraction of the ceramic phase of FG conical shells is considered to be linear, quadratic and inverse quadratic functions. The magnitudes of dimensionless excitation frequencies p_{11} and p_{12} for FG, pure metal and pure ceramic truncated conical shells decrease, as the dynamic axial load factor, T_{t1}, increases. As the dynamic axial load factor increases from 0 to 0.4, the values of the dimensionless excitation frequency, p_{11}, i.e., left boundaries of domains of dynamic instability for FG conical shells decrease, while the values of the dimensionless excitation frequency, p_{12}, i.e., right boundaries of domains of dynamic instability for FG conical shells increases. If the magnitudes of dimensionless excitation frequencies p_{11} or p_{12} for all kinds FG conical shells are compared with the corresponding values of the ceramic-rich conical shells, the influences of FG profiles remain constant, as T_{t1}, increases. When FG conical shells are compared with the corresponding ceramic-rich shells, the effects of FG profiles on the magnitudes of boundaries of domains of dynamic unstable of FG-A, FG-B, FG-C and FG-D truncated conical shells are (39.04%; 46.02%; 30.2%), (31.75%; 40.66%; 22.24%), (4.2%; 5.3%; 3%) and (4.23%; 5.92%; 2.67%), respectively for linear, quadratic and inverse quadratic profiles. It is observed that comparing the values of dimensionless excitation frequencies p_{11} or p_{12} for FG-A, FG-B,

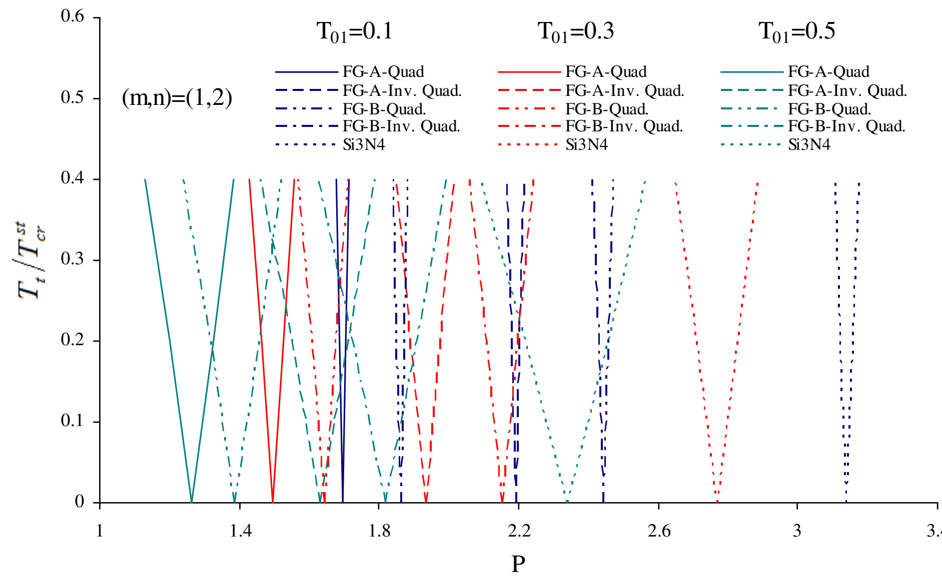

Fig. 2. Influence of variation of the static load factor, T_{01}, on the values of domain boundaries of dynamic instability for FG and fully ceramic conical shells.

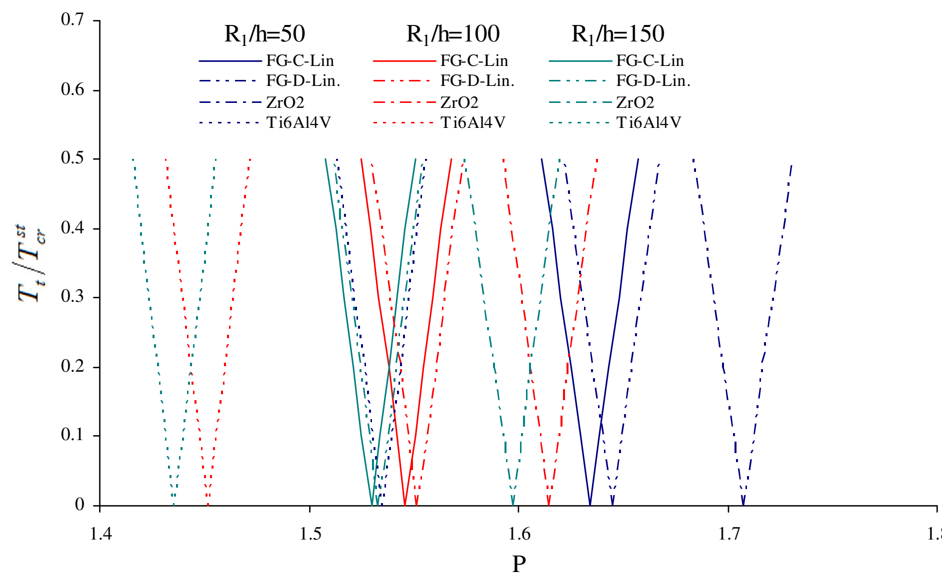

Fig. 3. Influence of variation of R_1/h, on the values of boundaries of domains of dynamic instability for FG-C, FG-D, ZrO_2 and Ti6Al4V.

FG-C and FG-D conical hells, the lowest value occurs in the FG-A conical shell and the highest value occurs in the FG-C conical shell.

5.2.2. Effect of the static axial load factor

The influence of variation of the static load factor, T_{01}, on the values of boundaries of domains of dynamic instability for FG-A, FG-B and Si_3N_4 conical shells are plotted in Fig. 2 show. The conical shell characteristics are taken to be $R_1/h = 100$; $L/R_1 = 2$; $\gamma = 30^\circ$ and the mode is $(m,n) = (1,2)$. The volume fraction of ceramic phase is considered quadratic and inverse quadratic functions. The domain of dynamic instability is bounded by two curves, originating from the same point of the axis p at $T_t = 0$ (see, Fig. 4). It is obvious that the values of the boundaries of domains of dynamic instability for conical shells decrease with increasing coefficient of static load, T_{01}. It is obvious also that the field of dynamic instability becomes gradually wider with increasing T_{01}. However, the slopes of domain boundaries increase with the increasing of the static axial load factor, T_{01} .The effects of FG profiles on the values of boundaries of domains of dynamic instability for FG conical shells remain constant, as the static axial load factor, T_{01}, increases. For example, the effects of quadratic and inverse quadratic profiles on the values of boundaries of domains of dynamic instability for FG-A shell are 46% and 30% and for FG-B shell are 41% and 22%, respectively, as T_{01} increases from 0.1 to 0.5. It is seen that the effect of FG-A profiles on the areas of dynamic instability of conical shells is more pronounced than that of the FG-B profiles.

5.2.3. Effect of the radius-to-thickness ratio

The influence of variation of the ratio, R_1/h, on the values of boundaries of instability domains for FG-C, FG-D, ZrO_2 and Ti6Al4V conical shells are shown in Fig. 3. The conical shell characteristics are; $L/R_1 = 2$ and $\gamma = 30^\circ$, the static axial load factor, $T_{01} = 0.1$ and mode is $(m,n) = (1,4)$. The volume fraction of the ceramic phase is taken to be linear function. It should be noted that the values of

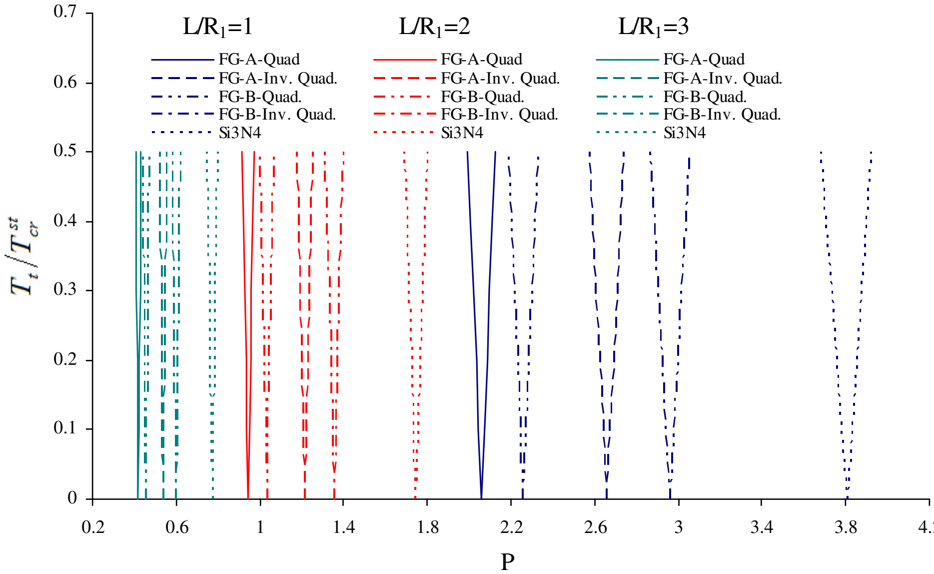

Fig. 4. Influence of variation of L/R_1, on the values of boundaries of instability domains for FG and pure ceramic conical shells.

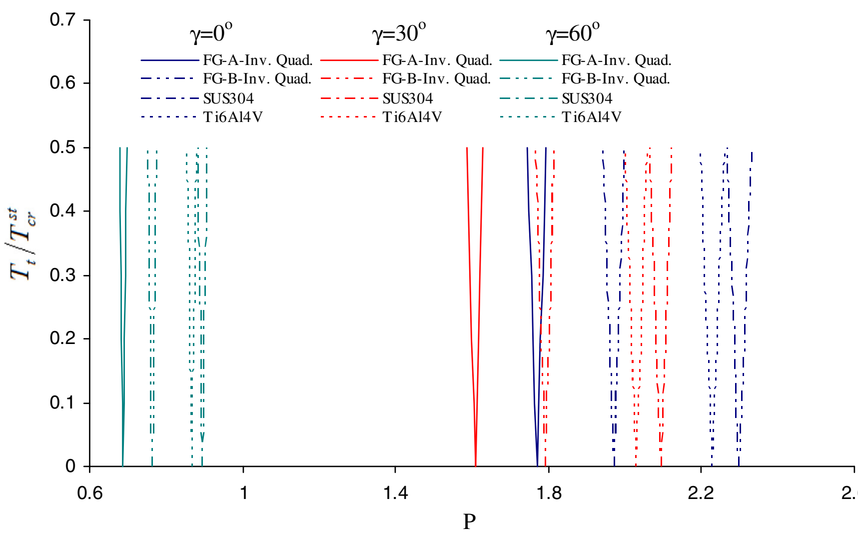

Fig. 5. Influence of variation of the semi-vertex angle, γ, upon the values of domain boundaries of dynamic instability for FG and pure metal shells.

boundaries of instability domains of conical shells decrease with the increasing of the ratio, R_1/h. The influence of the FG profiles on the values of boundaries of instability domains for conical shells is independent of the changes the ratio, R_1/h. For example, when FG-C-linear and FG-D-linear truncated conical shells are compared with the ZrO_2 and Ti6A14V truncated conical shells, respectively, the influences of FG-linear profiles on the values of boundaries of instability domains are 4.3% and 7%, respectively, as the ratio, R_1/h, increases from 50 to 150. It is also obvious that the sizes of instability regions decrease with the increasing of the dynamic axial load factor, while the sizes reduce with the increasing of the ratio, R_1/h.

5.2.4. Effect of the length-to-radius ratio

The influence of variation of the ratio, L/R_1, on the values of boundaries of instability domains for FG-A, FG-B and Si_3N_4 conical shells are illustrated in Fig. 4. The conical shell characteristics are, $R_1/h = 100$; $\gamma = 45^\circ$ and $(m,n) = (1,2)$. The static axial load factor are taken to $T_{01} = 0.2$, respectively. The volume fraction of the ceramic phase is quadratic and inverse quadratic. It is observed that the values of boundaries of instability domains of conical shells decrease monotonically, as L/R_1 increases from 1 to 3. The effects of FG profiles on the values of boundaries of instability domains for FG-A or FG-B conical shells remain constant, as the ratio, L/R_1, increases. For example, the effects of FG-quadratic and FG-inverse quadratic profiles are 46% and 30% respectively, as L/R_1 increases from 1 to 3. It is also observed that the sizes of the instability domains decrease with the increasing of the ratio, L/R_1.

5.2.5. Effect of the semi-vertex angle

The effects of the of variation of the semi-vertex angle, γ, upon the values of domain boundaries of instability of FG-A, FG-B, Ti6Al4V and SUS304 conical and cylindrical shells for mode (1,2) are analyzed. The cone semi-vertex angle with three values ($\gamma = 0^\circ, 30^\circ, 60^\circ$) are taken into account, and the results are shown in Fig. 5. Here $\gamma = 0^\circ$ corresponds to the cylindrical shell. The conical shell characteristics are; $R_1/h = 100$ and $L/R_1 = 2$. The volume fraction of ceramic phase is taken to be inverse-quadratic function and static load factor is $T_{01} = 0.1$. It is obvious that the values of domain boundaries of instability of conical shells decrease with the increasing of the semi-vertex angle, γ. It is obvious that the sizes of the instability domains decrease with the increasing the semi-vertex angle, γ. The effects of FG profiles on the values of boundaries of instability domains for FG-A or FG-B conical shells nearly remain constant, as the semi-vertex angle, γ, increases. For example, when FG-A and FG-B shells are compared with the SUS304 and Ti6A14V shells, respectively, the influences of FG-A-inverse quadratic and FG-B-inverse quadratic profiles on the values of boundaries of instability domains are 23% and 12%, respectively, as the semi-vertex angle, γ, increases from 0° to 60° with the step 30°.

6. Conclusion

The present study deals with the theoretical analysis of parametric instability characteristics of functionally graded (FG) conical shells subjected to harmonic axial loading based on the classical shell theory (CST). The basic relations and equations are derived using the Donnell shell theory. Appling Galerkin's method, the partial differential equations are reduced into a Mathieu type differential equation describing the dynamic instability behavior of the FG conical shell. Following Bolotin's method, the instability regions are determined from the boundaries of instability. Validation of numerical results was done with those available from previous researches. The influences of various parameters like static and dynamic load factors, volume fraction of FG profiles and shell characteristics on the dynamic instability domains of the truncated conical shells were investigated. Significant effects of these parameters on the dynamic stability characteristics of truncated conical shells were observed and discussed.

References

[1] Bolotin VV. The dynamic stability of elastic systems. San Francisco, CA: Holden-Day; 1964.

[2] Simitses GJ. Instability of dynamically loaded structures. Appl Mech Rev 1987;40:1403–8.

[3] Sahu SK, Datta PK. Research advances in the dynamic stability behavior of plates and shells: 1987–2005-Part I: conservative systems. Appl Mech Rev 2007;60:65–75.

[4] Nagai K, Yamaki N. Dynamic stability of circular cylindrical shells under periodic compressive forces. J Sound Vib 1978;58:425–41.

[5] Lam KY, Ng TY. Dynamic stability of cylindrical shells subjected to conservative periodic axial loads using different shell theories. J Sound Vib 1997;207:497–520.

[6] Lam KY, Ng TY. Parametric resonance of cylindrical shells by different shell theories. AIAA J 1999;37:137–40.

[7] Nawrotzki P, Kratzig WB, Montag U. Dynamic instability analysis of elastic and inelastic shells. Comput Mech 1998;21:48–59.

[8] Ng TY, Lam KY, Reddy JN. Parametric resonance of a rotating cylindrical shell subjected to periodic axial loads. J Sound Vib 1998;214:513–29.

[9] Pellicano F, Amabili M. Stability and vibration of empty and fluid-filled circular cylindrical shells under static and periodic axial loads. Int J Solid Struct 2003;40:3229–51.

[10] Han Q, Qin Z, Zhao A, Chu F. Parametric instability of cylindrical thin shell with periodic rotating speeds. Int J Non Linear Mech 2013;57:201–7.

[11] Han Q, Chu F. Effects of rotation upon parametric instability of a cylindrical shell subjected to periodic axial loads. J Sound Vib 2013;332:5653–61.

[12] Dey T, Ramachandra LS. Static and dynamic instability analysis of composite cylindrical shell panels subjected to partial edge loading. Int J Non Linear Mech 2014;64:46–56.

[13] Panda HS, Sahu SK, Parhi PK. Hygrothermal response on parametric instability of delaminated bidirectional composite flat panels. Eur J Mech Solid 2015;53:268–81.

[14] Kornecki A. Dynamic stability of truncated conical shells under pulsating pressure. Isr J Tech 1966;4:110–20.

[15] Tani J. Dynamic instability of truncated conical shells under periodic axial load. Int J Solid Struct 1974;10:169–76.

[16] Tani J. Influence of deformations prior to instability on the dynamic instability of conical shells under periodic axial load. J Appl Mech 1976;43:87–91.

[17] Tani J. Influence of deformation before instability on the dynamic instability of conical shells under periodic pressure. J Sound Vib 1976;45:253–8.

[18] Massalas C, Dalamangas A, Tzivanidis G. Dynamic instability of truncated conical shells, with variable modulus of elasticity, under periodic compressive forces. J Sound Vib 1981;79:519–28.

[19] Ng TY, Hua L, Lam KY, Loy CT. Parametric instability of conical shells by the generalized differential quadrature method. Int J Numer Meth Eng 1999;44:819–37.

[20] Ganapathi M, Patel BP, Sambandam CT, Touratier M. Dynamic instability analysis of circular conical shells. Compos Struct 1999;46:59–64.

[21] Kuntsevich SP, Mikhasev GI. Local parametric vibrations of a noncircular conical shell subjected to nonuniform pulsating pressure. Mech Solid 2002;37:134–9.

[22] Han Q, Chu F. Parametric instability of a rotating truncated conical shell subjected to periodic axial loads. Mech Res Commun 2013;53:63–74.

[23] Han Q, Chu F. Parametric resonance of truncated conical shells rotating at periodically varying angular speed. J Sound Vib 2014;333:2866–84.

[24] Koizumi M, Niino M. Overview of FGM research in Japan. MRS Bull. 1995;20:19–21.

[25] Reiter T, Dvorak GJ, Tvergaard V. Micromechanical models for graded composite materials. J Mech Phys Solid 1997;45:1281–302.

[26] Pindera MJ, Arnold SM, Abodi J. Use of composites in functionally graded materials. Compos Eng 1994;4:1–145.

[27] Suresh S, Mortensen A. Fundamentals of functionally graded materials. London: The Institute of Materials, IOM Communications Ltd; 1998.

[28] Kieback B, Neubrand A, Riedel H. Processing techniques for functionally graded materials. Mater Sci Eng A 2003;362:81–106.

[29] Naj R, Boroujerdy SM, Eslami MR. Thermal and mechanical instability of functionally graded truncated conical shells. Thin-Walled Struct 2008;46:65–78.

[30] Tornabene F, Viola E, Inman DJ. 2-D differential quadrature solution for vibration analysis of functionally graded conical, cylindrical shell and annular plate structures. J Sound Vib 2009;328:259–90.

[31] Zhao X, Liew KM. Free vibration analysis of functionally graded conical shell panels by a meshless method. Compos Struct 2011;93:649–64.

[32] Abediokhchi J, Shakouri M, Kouchakzadeh MA. Bending analysis of moderately thick functionally graded conical panels with various boundary conditions using GDQ method. Compos Struct 2013;103:68–74.

[33] Tornabene F, Viola E. Static analysis of functionally graded doubly-curved shells and panels of revolution. Meccanica 2013;48:901–30.

[34] Akbari M, Kiani Y, Aghdam MM, Eslami MR. Free vibration of FGM Lévy conical panels. Compos Struct 2014;116:732–46.

[35] Akbari M, Kiani Y, Eslami MR. Thermal buckling of temperature-dependent FGM conical shells with arbitrary edge supports. Acta Mech 2015;226:897–915.

[36] Heydarpour Y, Malekzadeh P, Aghdam MM. Free vibration of functionally graded truncated conical shells under internal pressure. Meccanica 2014;49:267–82.

[37] Malekzadeh P, Daraie M. Dynamic analysis of functionally graded truncated conical shells subjected to asymmetric moving loads. Thin-Walled Struct 2014;84:1–13.

[38] Su Z, Jin G, Ye T. Three-dimensional vibration analysis of thick functionally graded conical, cylindrical shell and annular plate structures with arbitrary elastic restraints. Compos Struct 2014;118:432–47.

[39] Selahi E, Setoodeh AR, Tahani M. Three-dimensional transient analysis of functionally graded truncated conical shells with variable thickness subjected to an asymmetric dynamic pressure. Int J Press Vessels Pip 2014;119:29–38.

[40] Viola E, Rossetti L, Fantuzzi N, Tornabene F. Static analysis of functionally graded conical shells and panels using the generalized unconstrained third order theory coupled with the stress recovery. Compos Struct 2014;112:44–65.

[41] Xiang X, Guoyong J, Tiangui Y, Zhigang L. Free vibration analysis of functionally graded conical shells and annular plates using the Haar wavelet method. Appl Acoust 2014;85:130–42.

[42] Nejad MZ, Jabbari M, Ghannad M. Elastic analysis of FGM rotating thick truncated conical shells with axially-varying properties under non-uniform pressure loading. Compos Struct 2015;122:561–9.

[43] Sofiyev AH. On the vibration and stability of shear deformable FGM truncated conical shells subjected to an axial load. Compos B Eng 2015;80:53–62.

[44] Sofiyev AH, Kuruoglu N. On a problem of the vibration of functionally graded conical shells with mixed boundary conditions. Compos B Eng 2015;70:122–30.

[45] Jam JE, Kiani Y. Buckling of pressurized functionally graded carbon nanotube reinforced conical shells. Compos Struct 2015;125:586–95.

[46] Ng TY, Lam KY, Liew KM, Reddy JN. Dynamic analysis of functionally graded cylindrical shell subjected under periodic axial loading. Int J Solid Struct 2001;38:1295–309.

[47] Ansari R, Darvizeh M. Prediction of dynamic behavior of FGM shells under arbitrary boundary conditions. Compos Struct 2008;85:284–92.

[48] Bespalova EI, Urusova GP. Identifying the domains of dynamic instability for inhomogeneous shell systems under periodic loads. Int Appl Mech 2011;47:186–94.

[49] Ovesy HR, Fazilati J. Parametric instability analysis of moderately thick FGM cylindrical panels using FSM. Comput Struct 2012;108–109:135–43.

[50] Lei ZX, Zhang LW, Liew KM, Yu JL. Dynamic stability analysis of carbon nanotube-reinforced functionally graded cylindrical panels using the element-free kp-Ritz method. Compos Struct 2014;113:328–38.

[51] Torki ME, Kazemi MT, Reddy JN, Haddadpoud H, Mahmoudkhani S. Dynamic stability of functionally graded cantilever cylindrical shells under distributed axial follower forces. J Sound Vib 2014;333:801–81.
[52] Sofiyev AH, Kuruoglu N. Dynamic instability of three-layered cylindrical shells containing an FGM interlayer. Thin-Walled Struct 2015;93:10–21.
[53] Shen HS. Functionally graded materials. In: Nonlinear analysis of plates and shells. Florida: CRC Press; 2009.
[54] Agamirov VL. Dynamic problems of non-linear shells theory. Moscow, Nauka, (in Russian); 1990.
[55] Li FM, Kishimoto K, Huang WH. The calculations of natural frequencies and forced vibration responses of conical shell using the Rayleigh–Ritz method. Mech Res Commun 2009;36:595–602.
[56] Kerboua Y, Lakis AA, Hmila M. Vibration analysis of truncated conical shells subjected to flowing fluid. Appl Math Model 2010;34:791–809.